

Benthic fluxes of methane along the salinity gradient of a tropical monsoonal estuary: Implications for CH₄ supersaturation and emission.

Jesly Araujo^{a*}, Anil Pratihary^a, Richita Naik^a, Hema Naik^a, S.W.A. Naqvi^{a,b}

^aChemical Oceanography Division, CSIR- National Institute of Oceanography,
Dona Paula, Goa 403004, India

^b Present address

Council of Scientific and Industrial Research, Rafi Marg, New Delhi 110 001, India

* Corresponding author: Email address: jess.araujo8@gmail.com

Abstract:

Observations in the Mandovi estuary, a typical tropical monsoonal estuary located on the west coast of India, revealed that waters were perennially supersaturated with CH₄, indicating that the estuary could be a significant emitter of this greenhouse gas. In order to test the hypothesis that the estuarine sediments serve as a major source of CH₄ to the overlying water column, a series of intact core incubations were carried out at three sites along the salinity gradient of the estuary during the summer (May–June) of 2014. The three sites - off Betim, Amona and Ganjem - represented different salinity regimes (33, 18 and 1, respectively). The benthic CH₄ fluxes exhibited a progressive increasing trend from 4.71 μmol m⁻² d⁻¹ at the marine end (S>20) to 16.01 μmol m⁻² d⁻¹ in the brackish water zone (20≥S≥5) and 93.90 μmol m⁻² d⁻¹ at the freshwater end (S<5). The total benthic flux of CH₄ from the Mandovi estuary was computed to be 9.79 x 10⁶ g y⁻¹. The observed upstream increasing trend may be controlled by a combination of salinity, sedimentary C_{org} and sediment cohesiveness. High rates of CH₄ oxidation (10–1364 μmol m⁻² d⁻¹) were observed at all the sites with an increasing trend upstream indicating salinity control on methanotrophy. Despite high methanotrophic activity at the sediment-water interface, the net benthic CH₄ release to the water column still remained significant, accounting for high CH₄ supersaturation of the estuarine water and making the estuary a potential CH₄ source to the atmosphere. Our result simply that during the monsoon (wet) season, benthic CH₄ fluxes may be even higher as the entire estuary becomes freshwater dominated.

Key words: Methane, Benthic flux, Salinity, Mandovi Estuary

1. Introduction:

Estuaries are dynamic ecosystems linking two contrasting biogeochemical regimes i.e. riverine and marine, and thus estuarine biogeochemistry is affected by mixing efficiency, residence time of estuarine water, varying salinity, and input of nutrients and organic matter (OM) from natural and anthropogenic sources. In estuaries with mangrove vegetation, and having proximal agricultural fields and human habitations, processing of OM and nutrients largely determines the estuarine biogeochemical characteristics, also influencing shelf biogeochemistry to some extent. Located at shallow depths, estuarine sediments receive large OM supply from diverse sources, and the efficiency, and pathway of OM mineralization determine the characteristic biogeochemical features and ecosystem functioning of an estuary.

Degradation of OM within the first few millimetres of the sediments takes place through aerobic oxidation and beneath the aerobic zone it proceeds anaerobically via sequential utilization of other electron acceptors in order of decreasing energy yield ($\text{NO}_3^- > \text{Mn}$ and Fe oxides $> \text{SO}_4^{2-} > \text{CO}_2$) (Canfield, 1993a,b). In contrast to shelf systems, lower salinity of estuarine water and consequently limited penetration of sulphate (SO_4^{2-}) into the estuarine sediments leads to methanogenesis occurring at a relatively shallower depth and can be a significant OM mineralization pathway in the estuarine sediments. These methane (CH_4)-rich sediments can serve as a significant source of CH_4 to the water column. Methane, a potent greenhouse gas (~25 times more powerful than CO_2) is known to be emitted from wetlands, paddy fields, mangrove swamps, shallow lakes and estuaries (Middelburg et al., 2002; Bridgman et al., 2013; Musenze et al., 2014).

Estuaries account for only about 0.4% of the global oceanic area (Bange et al., 1994), but can still be significant sources of CH_4 to the atmosphere (Lilley et al., 1995; Zhang et al., 2008). Being dynamic ecosystems, it is difficult to ascertain sources and sinks of CH_4 within an estuary. Nevertheless, recent studies have identified major sources and sinks, which include production in sediments, particularly at estuarine turbidity maxima (Martens 1982., Upstill-Goddard et al., 2000), input from tidal flats (Kelley et al., 1995; Middelburg et al., 2002), mangrove forests (Alongi et al., 2001) and agricultural fields (Sanders et al., 2007), CH_4 oxidation in surface sediment and in the water column (van der Nat et al., 1997; De Angelis and Scranton 1993), and emission to the atmosphere (Upstill-Goddard et al., 2000; Middelburg et al., 2002). The estuarine CH_4 concentrations vary over a wide range and show large temporal variations (Upstill-Goddard et al., 2000); and generally show an increasing pattern towards the freshwater end (Middelburg et al., 2002). In anoxic marine sediments, SO_4^{2-} availability allows sulphate-reducing bacteria to outcompete methanogenic bacteria (Capone

and Kiene, 1988) resulting in lower CH₄ concentrations in the top layers of the sediments where sulphate reduction occurs, which decreases downwards to a depth where SO₄²⁻ concentration reaches zero (Borges and Abril, 2011 and references therein). Furthermore, anaerobic oxidation of CH₄ (AOM) that occurs at the SO₄²⁻-CH₄ transition zone prevents CH₄ from diffusing upwards, thereby generating a concave-up CH₄ profile (Blair and Aller, 1995). Although CH₄ production and consumption within the sediments have been reported previously (Valentine, 2002; Knittel and Boetius, 2009), information on the role of sediment in controlling the CH₄ fluxes to the overlying water and subsequently to the atmosphere is inadequate. There is a lack of information on benthic CH₄ fluxes from tropical estuarine systems. Understanding CH₄ dynamics in tropical estuaries is important as the flow regime, temperature and OM input markedly vary from those of temperate estuaries.

The Mandovi estuary is a tropical estuary located on the central west coast of India. Like other west coast estuaries, the Mandovi estuary is also heavily influenced by the southwest (SW) monsoon during June to October. Heavy monsoonal rainfall causes massive fresh water discharge into the estuary from its large catchment area containing fringing mangrove forests, agricultural fields and human habitations. Although considered a relatively pristine estuary compared to many European and American estuaries, the causes of high CH₄ supersaturation (300 – 46,000 %) in the Mandovi estuarine water (Jayakumar et al., 2001; Rao and Sarma, 2016; Araujo et al., 2017) remain unknown. Such high CH₄ build-up in the Mandovi estuarine water could result from CH₄ inputs (1) from underlying sediments, (2) run-off from mangrove forests, (3) run-off from agricultural fields, and (4) waste discharge from human settlements. In the organic-rich Mandovi estuarine sediments, benthic CH₄ fluxes could be particularly significant.

In order to evaluate the role of estuarine sediment as a source of CH₄ in the estuarine water, we carried out a series of whole core incubations of estuarine sediments along the salinity gradient during May – June 2014. In previous studies conducted elsewhere, benthic CH₄ fluxes were either computed from porewater CH₄ profiles (De Angelis and Scranton 1993; Huttunen et al., 2006), or measured directly using benthic chambers (Martens and Klump 1980; Sansone et al., 1998; Kelley et al., 1990; Deborde et al., 2010; Bednarik et al., 2015) and whole-core incubations (Abril and Iverson 2002; Zhang et al., 2008). As the benthic fluxes measured by whole-core incubations can be very similar to those obtained through benthic chamber incubations (Miller-Way et al., 1994; Hammond et al., 2004; Woulds et al., 2009), we preferred the former method to quantify CH₄ fluxes due to

logistic convenience. To our knowledge, this is the first ever attempt to quantify benthic CH₄ fluxes directly in any Indian estuary.

2. Material and methods

2.1. Study area

The Mandovi River originates in the Western Ghats that form the western boundary of the narrow western coastal plain of India and flows nearly 75 km through the state of Goa before meeting the Arabian Sea. The estuary of this river is located between latitudes 15° 27' and 15°31'N, and between longitudes 73° 45' and 73° 59'E. It is a shallow estuary (depth ~ 5 m) that remains well-mixed during most parts of the year except during the SW monsoon when the water column remains partially stratified close to the estuarine mouth. The estuary covers an area of ~29 km² and can be divided into two regions based on its geographical features, i.e. the bay and channel. The Aguada Bay (mouth region) is ~ 3.2 km wide, and the channel rapidly narrows down to ~ 0.25 km upstream. The estuary has a large catchment area (1,150 km²) comprised of fringing mangrove forests, agricultural lands and human habitations. Several smaller streams carrying OM and nutrients, and weathered material from the Western Ghats drain into the estuary. The Western Ghats, running parallel to the west coast at an average elevation of ~1 km, cause heavy rainfall during the SW monsoon over the western coastal plains in the states of Maharashtra, Goa, Karnataka, and Kerala. The estuary receives $1,689 \times 10^6$ m³ (June – September) of fresh water discharge compared to $74 - 19 \times 10^6$ m³ during the dry season (November–May). As a result, the estuary experiences extreme seasonal variability with nearly freshwater conditions prevailing during the summer (SW) monsoon *i.e.* June to September (Vijith et al., 2009). The water column is partially mixed after the monsoon (October–January) due to the decrease in rainfall and river influx, and well-mixed conditions prevail during the pre-monsoon period (February–May). The Mandovi estuary is a macro-tidal estuary experiencing semi-diurnal tides (tidal range ~ 1.5 to 2.3 m). During the pre-monsoon season, the estuary remains tide-dominated with seawater intruding up to ~ 55 km upstream. The estuary develops a prominent salinity gradient along the length of estuary at this time. The residence time of estuarine water during the SW monsoon has been reported to be 2 days which increases to 31 days in the dry season (<http://nest.su.se/mnode/Asia/India/Mandovi/Mandovibud.htm>). The estuary is used for industrial, agricultural and tourism purposes, and hence receives wastes from industries, agricultural fields, human activities like fishing, transport of iron and manganese ore by barges, passenger ferries, and recreational activities like boat cruises for tourists (Maya et al., 2011). Although the estuary also receives waste discharges from mining industries and treated municipal

sewages at some points, it is still considered as a relatively pristine estuary compared to many European and American estuaries. This is evident from the relatively low concentrations of NO_3^- ($\leq 10\mu\text{M}$), NH_4^+ ($\leq 4\mu\text{M}$) and PO_4^{3-} ($\leq 1\mu\text{M}$) in the estuarine water (Maya et al., 2011).

2.2. Selection of sampling sites and core collection.

In the present study, the Mandovi estuary was divided into three zones based on salinity (S): (1) the marine dominated or high salinity zone ($S > 20$), (2) the brackish water or mid-salinity zone ($20 \geq S > 5$), and (3) the freshwater-dominated zone ($S \leq 5$). Since the estuary receives negligible freshwater input during the pre-monsoon, the salinity ranges at the mouth region ($S > 20$), mid-estuary ($20 \geq S > 5$) and upstream region ($S < 5$) remain nearly the same irrespective of tidal condition as per our previous observation. Representative stations were selected for the three zones; these were located at Betim ($15^\circ 30.326' \text{N}$; $73^\circ 49.796' \text{E}$), Amona ($15^\circ 31.573' \text{N}$; $73^\circ 58.143' \text{E}$) and Ganjem ($15^\circ 28.133' \text{N}$; $74^\circ 05.596' \text{E}$), where the salinity was around 33, 18 and 1 respectively (Fig. 1). Sampling was carried out at these sites during the low tide between May 22nd to June 6th, 2014 when the estuary was vertically well-mixed and well-oxygenated and the salinity gradient along the length of the estuary was well-established. The tidal range on the day of the sampling varied between 0.72 to 1.99 m; 0.8 to 1.83 m and 0.15 to 2.09 m at Betim, Amona and Ganjem, respectively. Five sediment cores were collected carefully with minimal disturbance by using specially designed (Fig.2) Plexiglas core liners (length: 48cm, ID: 10.1cm, thickness: 0.5 cm) within 1 m² area. About 10 litres of estuarine bottom water was also collected in plastic carboys for use in the incubation experiments. Three additional sediment cores - one for porosity, grain size and organic carbon (C_{org}), and the other two for pore water analyses - were collected in 6.4 cm ID and 30 cm long bevelled Plexiglas core liners. All the cores were immediately covered with aluminium foil to protect them from light exposure and quickly transferred to the air-conditioned laboratory at National Institute of Oceanography. The overlying water was also kept in the dark in the air-conditioned laboratory.

2.3. Intact core incubations and sampling

The core incubations were carried out following a procedure modified from Pratihary et al. (2014). The overlying water was slowly poured over the five incubation cores without disturbing the surficial sediments. The cores were then aerobically pre-incubated for 24h in the dark in a temperature controlled laboratory, which was maintained close to the in-situ conditions ($\pm 0.5^\circ\text{C}$). After pre-incubation, the overlying water was carefully siphoned out and replaced carefully by fresh overlying water. Core A and core B (duplicates) were incubated anaerobically. Core C and core D (duplicates) were incubated aerobically i.e. the overlying water was continuously aerated using an electrically

operated aerator. In core E, the overlying water was poisoned by HgCl_2 and it was incubated anaerobically. The estuarine overlying water was also put into two aluminium-coated trilaminate gas-tight bags with volumes of 5L (Bag A) and 1.5L (Bag B). The headspace was removed in both the bags. The water in Bag B was poisoned with HgCl_2 and was connected to core E. Bag A was incubated anaerobically along with the cores. The overlying water also put into a specially designed Nalgene plastic bottle (Bottle A) which was aerobically incubated along with the cores. The incubations of all sediment-water and water samples were continued for 5 days. The experimental set up for the intact core incubation is shown in Fig.2.

The overlying water was sampled at 6h intervals, initially and later at 12h intervals using a glass or plastic syringe, pre-flushed with N_2 , through tubing connected at the middle of the core liners. Dissolved oxygen (DO) samples were collected in He-flushed 5 ml Hamilton gastight syringes and were fixed using Winkler reagents. CH_4 samples were collected in He-flushed 60 ml plastic syringes and transferred into a 15ml glass vial followed by immediate poisoning by adding 100 μL of saturated HgCl_2 solution and were crimped using butyl septa without trapping any air bubble. In case of core A and core B, the sample drawn was replaced by estuarine bottom water from Bag A connected to the cores through the tubing at the middle of the core liners. In case of core C and core D, the sample drawn was replaced by water from the Bottle A, and in case of core E, the sample drawn was replaced by poisoned bottom water from Bag B.

2.4. Sample analyses

DO samples were acidified by adding 50% H_2SO_4 and were analysed spectrophotometrically (Pai et al., 1993). Methane was analysed using a Shimadzu gas chromatograph equipped with a flame ionisation detector following McAuliffe (1971) with a precision better than 4%. Briefly, 15 ml of sample was equilibrated thrice successively with an equal volume of high purity helium (He) in an air-tight syringe for 5 min on a mechanical equilibrator (Griffin flask shaker wrist action). The equilibrated headspace was injected into a gas chromatograph (Shimadzu GC 2010 Series) through a sampling loop after passing over a moisture trap (activated drierite). Separation was achieved over a stainless steel column (1.8 m length, 3.2 mm diameter) packed with molecular sieve 5A (mesh 80/100) and maintained at a temperature of 60°C. Calibration was carried out using standard gas mixtures and air samples (1777 ppb CH_4) were frequently run to monitor the detector response.

For measurements of porosity, C_{org} and grain size, the core was sectioned at 1cm interval. A portion of sediment samples was weighed and oven dried at 60°C. After homogenization of sediments, the porosity was then determined following the protocol described in Pratihary et al. (2014). For C_{org} , a

portion of sediment samples was freeze dried, homogenized, and analysed for total carbon (TC) and inorganic carbon (IC). The TC content was determined using an elemental analyser (Thermo Flash EA 1112 series) with a precision of <0.8%. The sedimentary IC content was determined using a UIC Carbon Coulometer (CM 5015) with a precision better than 3%. C_{org} content was calculated as the difference between TC and IC. For grain size analysis, a part of sediment samples was oven-dried at ~50 °C and sieved using ISTM 230 mesh sieve to separate the sand fraction (< 2000 µm – > 63 µm) from clay and silt. The sand fraction retained on the sieve was collected, dried and weighted. The < 63 µm fraction was analysed by a Malvern Laser Particle size analyzer (Master sizer 2000) for silt and clay. Thereafter the weight percentages of sand (< 2000 µm – > 63 µm), silt (< 63 µm – > 4 µm) and clay (< 4 µm) were calculated as per Folk (1968).

2.5. Porewater extraction and analysis

For porewater SO₄²⁻ analysis, porewaters were extracted at 1cm interval through Rhizon tubings (Rhizosphere Research Products, Wageningen, The Netherlands) following Seeberg-Elverfeldt et al. (2005). Sulphate was analysed by anion exchange chromatography with suppressed conductivity detection using an Ion Chromatograph (Dionex, ICS 5000). The precision of analysis was better than ± 0.05 mM. Aliquots of the extracted porewater were also used to measure porewater salinity using an Atago refractometer with a precision of ± 2 ppt. Samples for hydrogen sulphide (H₂S) were extracted in gas tight Hamilton glass syringes and analysed following Cline (1969). The precision of this method was around ± 0.14 µM.

Porewater extraction for CH₄ was carried out in a glove box that was continuously flushed with N₂. Each core was sectioned at 1 cm interval and the sediment slice was transferred into N₂-flushed 60 ml Wheaton bottles containing 5ml of 40% ZnCl₂ to bind sulphide. Thereafter 1ml of saturated HgCl₂ was added to inhibit microbial activity and the bottle was filled up with degassed estuarine bottom water without trapping any air bubble. The Wheaton bottles containing the sediment slurry were mixed well and the sediment was allowed to settle down. The overlying water was then drawn into a syringe and analysed as described in section 2.4.

2.6. Flux calculation and statistical analysis

Sediment-water CH₄ flux was calculated following Pratihary et al. (2009)

$$F (\mu\text{mol m}^{-2} \text{d}^{-1}) = \frac{V}{A} \times \frac{dC}{dt} \times \frac{24}{1000}$$

Where V is the volume (L) of overlying water in the core.

A is the surface area (m²) of sediments underlying the water column in the core and

$\frac{dC}{dt}$ is the slope of the linear regression of CH₄ concentration (nM) versus time (h)

Positive F values represent flux from sediment to water while negative values represent loss of CH₄ from water.

Linearity of CH₄ accumulation with incubation time was examined by Pearson's correlation test (MS excel) and correlation factor (r) was used to indicate a strong or poor correlation. Parametric single factor ANOVA (MS Excel) was applied between CH₄ datasets of anaerobic and aerobic cores, to assess the variance in CH₄ accumulation between two replicate and non-replicate cores. Correlation between other parameters was also analysed by Pearson's correlation test. The threshold value for statistical significance was considered to be $p < 0.05$.

3. Results

3.1 Water column and sediment characteristics

As the observations were made during the pre-monsoon season, the water column was well-mixed and the salinity gradient was well-established. Depending upon the tidal variations described earlier, the depths of the sampling stations ranged between 4 – 6 m at Betim, 7 – 9 m at Amona and ~ 1 m at Ganjem. Temperature varied within a narrow range from 29 to 32 °C, and the salinity decreased from around 33 ppt at Betim to 18 ppt at Amona and to 1 ppt at Ganjem. The DO was 154 µM at Betim, 151 µM at Amona and 165 µM at Ganjem. The generally increasing trend has also been reported previously by Qasim and Sen Gupta (1981) and De Sousa and Sen Gupta (1986), and ascribed to greater gas solubility in fresher water. As expected, SO₄²⁻ exhibited a decreasing trend: 25 mM at Betim, 16 mM at Amona, and 0.01 mM at Ganjem. The water column CH₄ concentration was 28 nM, 140 nM and 360 nM respectively at the three sites.

The porewater constituents reflected the salinity gradient in the overlying waters, although porewater salinity (data not shown) was somewhat higher than that in the overlying water at all stations, probably due to residual high salinity water during high tide and/or evaporation during the low tide. However, within the cores, salinity changes were not very large. Porewater SO₄²⁻ concentrations varied between sites, obviously reflecting the salinity distribution along the length of the estuary. Porewater SO₄²⁻ at Betim varied from 25.18 to 23.24 mM, while at Amona it ranged from 15.32 to 17.26 mM, and at Ganjem the concentrations were between 0.01 and 2.74 mM (Fig. 4b). The organic carbon content of the sediment increased towards the freshwater end, being 1.72 – 3.51%, 2.19 –

4.67%, and 6.35 – 8.51% at Betim, Amona and Ganjem, respectively (Fig. 4a). The sediment texture also varied between the sites, with an overall higher silt content at all the stations (Fig.3 b,c,d). The sediment porosity increased from 0.58 to 0.64 at Betim to a rather constant value of ~ 0.7 at Amona and Ganjem with the exception of a layer at 12–16 cm at Amona where a band of sand was found, which reduced the porosity (Fig. 3a). Porewater sulphide concentration (data not shown) did not show any significant pattern along the salinity gradient. It was often below detection in most cores, especially at Amona, and the maximal values did not exceed 1 μM at Betim and Ganjem. Such low levels of sulphide despite substantial SO_4^{2-} in the porewater suggests that sulphide produced through SO_4^{2-} reduction was probably bound as insoluble sulphides, mainly Fe (pyrite), as the sediments are rich in Fe and Mn. Porewater CH_4 increased towards the freshwater end. At Betim porewater CH_4 varied from 2 μM in the upper few centimetres to a maximum of 24 μM at 10 cm and a decreased thereafter to 3 – 4 μM at deeper levels. At Amona, the porewater CH_4 increased from 2 μM at the surface to a maximum of 96 μM at 11cm, decreasing progressively thereafter with depth. As expected, the maximal porewater CH_4 build-up was observed at the freshwater end (Ganjem), where CH_4 increased from 435 μM in the surficial sediments to 9,529 μM at 15 cm (Fig. 4c).

3.2 Variability of dissolved constituents and fluxes across the sediment-water interface

3.2.1 Betim

Dissolved Oxygen

The dissolved oxygen in the overlying waters decreased steadily with time in the closed cores (A and B) (Fig.5a). At the beginning of the experiment the overlying water in both the cores was well-oxygenated (DO=202 μM). DO decreased substantially within the next 30h (to 64 μM in core A, and 42 μM in core B) reaching near suboxic levels within 60h (8 μM in core A, and 11 μM in core B). No significant variability was observed ($p>0.05$) between the DO decrease patterns between the two cores. In core E, the initial DO concentration was 189 μM which also decreased with time, but more slowly to 48 μM at the end of the experiment (120 h). A similar trend was observed in Bag A. However, as expected, the overlying waters remained well oxygenated in core C (221–259 μM), core D (227–257 μM) and Bottle A (216–229 μM) throughout the experiment. The variation in the decreasing pattern of DO in the aerobic cores (C and D) were statistically insignificant ($p= 0.5$).

Methane

The CH_4 concentration in the overlying water column increased with time (Fig. 5b). The initial CH_4 concentrations in both the cores were similar (25 nM in core A, 22 nM in core B). The concentration

decreased slightly in both the cores over the first 24 h (to 22nM in core A, 17nM in core B). After 36h, CH₄ began accumulating linearly in both the cores and this trend persisted until the end of the experiment. The variation between the CH₄ increase pattern in the anaerobic cores (A and B) was statistically insignificant ($p > 0.05$). Core E showed a clear and large increase in CH₄ concentration from 16 nM to 479 nM during the course of the experiment. The CH₄ concentration in cores C and D, and in Bottle A varied non-linearly within a narrow range (~3 – 10 nM), but the concentration in Bag A increased to 97 nM. The difference in CH₄ variability between cores C and D was statistically insignificant ($p > 0.05$).

3.2.2 Amona

Dissolved Oxygen

In the cores collected at Amona the initial DO concentrations were 212 μ M in core A and 241 μ M in core B. Within 24 h of incubation the concentrations decreased to 77 μ M and 73 μ M respectively, and were close to detection limit after 60 h (4 and 3 μ M in cores A and B, respectively) (Fig. 6a). In core E, the initial DO concentration was 236 μ M that fell to 55 μ M by the end of the experiment. DO concentration also declined from 242 μ M to 164 μ M in Bag A. High DO concentrations persisted in core C (221 – 306 μ M) and core D (242 – 284 μ M) and Bottle A (243 – 285 μ M). The DO concentration changes did not vary significantly between cores A and B ($p > 0.05$), and between cores C and core D ($p > 0.05$).

Methane

Dissolved CH₄ concentration increased linearly to different levels in cores A and B (Fig.6b). Initially the overlying water in core A contained 70 nM CH₄, whereas in core B the concentration was 45 nM. Although DO decreased with time in both cores, the final CH₄ concentration was much higher in core A (924 nM) than in core B (345 nM). The variation in the CH₄ accumulation pattern in core A and core B, was statistically significant ($p < 0.05$), the reasons for which will be discussed in section 3.3. In core E, CH₄ accumulated linearly and at much faster rate with time, as compared to core A and core B, from an initial concentration of 46 nM to a final concentration of 538 nM. A smaller increase occurred in Bag A (81–124 nM). The open (aerobic) cores, on the other hand, showed little change, with CH₄ levels ranging from 4 to 21 nM, and no significant difference ($p = 0.5$) between CH₄ concentrations of the two cores. Similarly, in Bottle A CH₄ concentrations were between 2 and 38 nM.

3.2.3 Ganjem

Dissolved Oxygen

The initial DO concentrations in overlying waters of cores A and B were 227 μM and 232 μM , respectively. The DO was depleted sharply with time to 92 μM in core A and 84 μM in core B after 32 h, decreasing further to undetectable levels (Fig.7a). The variation in the DO decrease pattern in cores A and B was not statistically significant ($p = 0.5$). In core E the initial DO value was 202 μM decreasing to 25 μM at the end of the experiment. DO concentrations in cores C and D and in Bottle A remained high (259 – 309 μM , 259 – 298 μM and 240 – 288 μM , respectively). No statistically significant difference ($p > 0.05$) was observed between cores C and D. The DO decline in Bag A was much more modest (from 250 μM to 215 μM) as compared to the other two locations.

Methane

Ganjem being at the freshwater end of the estuary, initial CH_4 concentrations were higher at this station (462 nM in core A, 307 nM in core B) than at Betim and Amona. The concentrations increased linearly with time during incubation to 1,895 nM in core A and 1,307 nM in core B at 26 h. However, no significant changes were observed in both cores until 62 h where the concentration of CH_4 in core A was 1,919 nM and core B was 3,408 nM. Towards the end of the experiment *i.e.* at 110 h, the CH_4 concentration in core B (11,137 nM) was almost five times that in core A (2,415 nM) (Fig. 7b), probably due to ebullition which is discussed in section 3.3. Therefore the variation in the CH_4 concentration in core A and core B was significant ($p < 0.05$). A much higher increase occurred in core E. The initial concentration was 2,904 nM that increased to 24,655 nM after 26 h, reaching up to 37,969 nM at the end of the experiment. The difference in CH_4 between aerobic cores C and D was statistically significant ($p < 0.001$). In core C (5 – 20 nM), core D (27 – 81 nM), Bag A (126 – 318 nM) and Bottle A (3 – 201 nM) overall higher ranges of dissolved CH_4 were seen as compared to the other two sites.

3.3. Methane flux rates

No significant increase in CH_4 was observed in Bag A at all three sites in contrast to anaerobic cores (Core A and B) wherein CH_4 built up linearly with time. This clearly indicated that the accumulated CH_4 in the overlying water came from sediments rather than being generated within the water column. Benthic CH_4 fluxes computed from cores A and B at Betim averaged 4.71 $\mu\text{mol m}^{-2} \text{d}^{-1}$; for core C and D the average flux was $-0.06 \mu\text{mol m}^{-2} \text{d}^{-1}$ while for core E it was 21.80 $\mu\text{mol m}^{-2} \text{d}^{-1}$. At Amona, the CH_4 flux varied from 67.64 $\mu\text{mol m}^{-2} \text{d}^{-1}$ in core A to 16.01 $\mu\text{mol m}^{-2} \text{d}^{-1}$ in core B. In

cores C, D and E the average values were $-0.71 \mu\text{mol m}^{-2} \text{d}^{-1}$, $-0.41 \mu\text{mol m}^{-2} \text{d}^{-1}$, and $26.31 \mu\text{mol m}^{-2} \text{d}^{-1}$, respectively. At Ganjem, the flux averaged $93.90 \mu\text{mol m}^{-2} \text{d}^{-1}$ in core A, $508 \mu\text{mol m}^{-2} \text{d}^{-1}$ in core B, $-0.23 \mu\text{mol m}^{-2} \text{d}^{-1}$ in core C, $-1.94 \mu\text{mol m}^{-2} \text{d}^{-1}$ in core D and $1458 \mu\text{mol m}^{-2} \text{d}^{-1}$ in core E. Thus, the benthic fluxes of CH_4 in the aerobic cores (core C and core D) at all the stations were negative, indicating CH_4 consumption/loss through enhanced aerobic oxidation in the overlying water column and/or air bubbling. The consistency in CH_4 flux rates between Core A and Core B at Betim suggested a credible reproducibility of flux rates and minimal spatial heterogeneity within a particular salinity zone. At Amona and Ganjem, although variance of DO concentrations between duplicate anaerobic cores (A and B) was statistically insignificant ($p>0.05$) suggesting a good replication, considerable differences in CH_4 fluxes between these two cores were observed. This could be largely attributed to CH_4 ebullition observed in core A of Amona (encircled values; Fig.6b) and core B of Ganjem (encircled values; Fig.7b) during the course of the incubation. Extremely high CH_4 build-up in the headspace of these cores (Fig.6b.1; Fig.7b.1) substantiated the massive ebullition of CH_4 from the sediments. Ebullition occurs when the production of CH_4 raises the sum of the partial pressures of the dissolved gases above the hydrostatic pressure in the sediment (Chanton and Dacey, 1991). The gaseous CH_4 content of sediments depends on various factors such as the flux of OM deposited at the sediment surface, reactivity of sedimentary OM, availability of SO_4^{2-} to support sulphate reduction, oxidation of CH_4 in the sulphate reduction zone, solubility of CH_4 at in situ conditions, and the rate of transport of CH_4 from the sediment via ebullition (Martens et al., 1998).

Methane ebullition resulted in headspace formation just below the Nylon cap in these cores. The headspace CH_4 was measured at 6, 42, 66, and 90 h for Amona and at 13, 26, 50, 62, 74, 86, 98, and 110 h for Ganjem. Headspace CH_4 concentrations were very high and increased with time (Fig. 6b.1 and Fig 7b.1). Accordingly, CH_4 concentrations in the overlying water of these two cores were also very high. Therefore, core A at Amona and core B at Ganjem were not considered for the calculation of the benthic flux of CH_4 , as the rates would be overestimated. To the best of our knowledge there are no reports of in-situ CH_4 ebullition in the Mandovi estuary, but it probably occurs, as reported from many other estuaries around the globe (Martens and Klump, 1980; Chanton et al., 1989; Middelburg et al., 1996), contributing to benthic CH_4 fluxes. The differences in CH_4 fluxes between duplicate cores (A and B) at Amona and Ganjem could also be due to spatial heterogeneity to some extent.

4. Discussion

4.1. Sediment-water CH_4 exchange and its controlling factors

Methane build-up within the sediments is a resultant of its production through fermentative anaerobic methanogenesis and its anaerobic/aerobic oxidation by SO_4^{2-} , NO_2^- and O_2 (Knittel and Boetius, 2009). As porewaters become supersaturated with CH_4 , it leads to a strong concentration gradient across the sediment-water interface triggering diffusive transport of CH_4 to the water column. In addition, benthic CH_4 fluxes are also facilitated by benthic faunal activity and ebullition. In the present study, we did not see any significant linear increase in CH_4 in the anaerobic bags (Bag A) but there was substantial linear CH_4 accumulation in the anaerobic cores (Core A and B) which indicates CH_4 release from sediments rather than production within the water column. Methane flux in these cores was always directed from the sediments to the overlying water, which is mainly due to high CH_4 production in the porewaters which led to a strong concentration gradient across sediment-water interface. In addition, benthic faunal activity probably also facilitated gas exchange across sediment-water interface. Methane ebullition from the sediments is episodic and patchy depending on sedimentary C_{org} , porosity, granulometry, and the CH_4 flux due to ebullition rates are non-steady and non-linear. Although such fluxes may not be considered for representative rate calculations, they can certainly lead to higher CH_4 accumulation in the estuarine water. Disproportionate CH_4 build-up in the overlying water and in the headspace (Fig.6b.1 and 7b.1) in one of the anaerobic cores at Amona and Ganjem and the observed gas ebullition shows that there is a high possibility of CH_4 ebullition from the estuarine sediments in the natural environment though it can be patchy and intermittent.

The CH_4 fluxes across the sediment-water interface varied significantly along the salinity gradient (Fig. 8a). This variation could be due to a combination of several factors such as the ambient temperature, SO_4^{2-} availability, sediment texture, porosity, organic carbon content, microbial activity and benthic faunal activity at the sediment/water interface (Huttunen et al., 2006). Strong biogeochemical gradients were observed along the length of the Mandovi estuary during the studied period. The upstream decrease in salinity was reflected in the decrease in porewater SO_4^{2-} concentration from Betim to Ganjem (Fig.4a). The organic carbon content of sediments increased towards the freshwater end (Fig.4b) possibly due to higher OM inputs from the catchment area. Although sediment porosity did not vary drastically between Betim and Amona (70 – 80%), sediment cohesiveness (silty-clayey %) progressively increased towards the freshwater end (Fig.3).

The highest benthic CH_4 flux rate was observed at Ganjem ($93.90 \mu\text{mol m}^{-2} \text{d}^{-1}$); the rate was moderately high at Amona ($16.02 \mu\text{mol m}^{-2} \text{d}^{-1}$) while the lowest rate was measured at Betim ($4.71 \mu\text{mol m}^{-2} \text{d}^{-1}$). Such spatial variation in fluxes could be due to interplay of several factors such as C_{org}

content, porosity, granulometry, porewater SO_4^{2-} , microbial activity and benthic faunal activity in the estuarine sediments. The OM (*i.e.* C_{org}) content is an important factor facilitating methanogenesis in sediments (Reshmi et al., 2014). Studies carried out elsewhere have shown that the porewater CH_4 concentration is positively correlated with the amount of OM and cohesiveness (fine granulometry) of sediments (Gar'kusha et al., 2010; Baulch et al., 2011). This seems to also apply for the Mandovi estuary where high percentage of fine (silty-clayey) sediments along with high organic carbon content occur at the freshwater end where the porewater CH_4 concentrations are also the highest. Wafar et al. (1997) reported maximum litter fall into the mangrove wetlands during the dry season, which may be an important source of labile OM to the estuarine sediments supporting CH_4 production. The $\delta^{13}\text{C}$ of terrestrial plants ranges from -24‰ to -34 ‰ and that of marine organic carbon ranges from -12‰ to -23 ‰ (Smith and Epstein 1971). The $\delta^{13}\text{C}$ values for sediments of the Mandovi estuary shows that OM source was dominantly terrestrial (R. Naik et al. *manuscript in preparation*). We observed a progressive increase in porewater CH_4 concentration and benthic CH_4 fluxes from Betim to Ganjem which were strongly correlated ($r^2=0.97$) with sedimentary C_{org} (Fig.8c). Thus, higher C_{org} in the sediments towards the upstream region apparently contributed to high rate of methanogenesis in the porewaters and fluxes into the water column.

As expected, porewater CH_4 concentrations decreased towards the marine end of the estuary which could be attributed to inhibition of CH_4 production by higher SO_4^{2-} availability in the porewaters towards the mouth region as observed elsewhere (Dutta et al., 2015). As mentioned earlier, a spike in the CH_4 profile was observed between, 10–11cm in the core at Betim, which coincided with a minimum in the porewater SO_4^{2-} (21.03 mM). This indicated that SO_4^{2-} availability affected methanogenesis. This was further evidenced by a strong negative correlation of porewater CH_4 and CH_4 flux rates with porewater SO_4^{2-} (Fig.8b). The competition between sulphate reduction and methanogenesis is driven by various microbial and physical factors (Martens et al., 1998). When SO_4^{2-} concentration drops below the threshold necessary to sustain microbial sulphate-reducing activity, OM remineralization continues via methanogenesis (Martens et al., 1998). At Ganjem, CH_4 concentration increased to a maximum value of 9,529 μM at a depth of ~15 cm, where the sulphate reduction rate was also at its maximum (R. Naik et al., *manuscript in preparation*). Martens and Berner (1974) have reported greater CH_4 production in freshwater areas because the low SO_4^{2-} concentrations in freshwaters. Experimental studies have also demonstrated that sediments rich in organic carbon and having porewater $\text{SO}_4^{2-} < 60\mu\text{M}$ may favor simultaneous occurrence of SO_4^{2-} reduction and CH_4 production, leading to high accumulation of porewater CH_4 (Deborde et al., 2010 and references therein). Methane produced can be oxidized under both aerobic and anaerobic

conditions (Kruger et al., 2005; Treude et al., 2005). As demonstrated by Jørgensen et al. (2001), the upward diffusing CH_4 is oxidized to CO_2 by SO_4^{2-} , which amounts to a SO_4^{2-} loss equivalent to about 10% of the total SO_4^{2-} reduction in coastal sediments. Thus, SO_4^{2-} plays an important role in controlling the CH_4 concentration/fluxes in/from the sediments.

During the pre-monsoon season the Mandovi estuary offers favourable conditions for high primary production (Krishna Kumari et al., 2002) due to low turbidity and is therefore net autotrophic (Pradeep Ram et al., 2003). Although during this season the riverine supply of nutrients remains low (Maya et al., 2011), high benthic nutrient fluxes to the water column (Pratihary et al., 2009) sustain high primary productivity which probably leads to high particulate organic carbon flux to sediments. In addition, extraneous OM also enters the estuary through run-off from mangrove forests, agricultural lands and human settlements supporting benthic fauna in the estuarine sediments. Ansari and Parulekar (1993) reported high macrofaunal abundance in the sediments of the Mandovi estuary. Activity of these benthos is expected to promote exchange of dissolved constituents across the sediment-water interface and aeration of the upper sedimentary layer. Higher biomass of bivalves especially molluscs have special affinity towards sandy substratum while polychaete preference for mud-dominated sediments at the upstream stations has been reported by Ansari et al. (2007). Thus, bioturbation and bioirrigation also possibly enhanced CH_4 release from the estuarine sediments as observed by Longhi et al (2013) elsewhere.

Cohesive sediments tend to hold higher C_{org} compared to permeable sediments. This was conspicuous in our study as C_{org} and silt-clay percentage of sediments increased simultaneously from Betim to Ganjem. The increase in the silt-clay content of the sediments, coupled with increase in C_{org} content towards the freshwater end reduced the permeability of the sediments thereby restricting the O_2 penetration and in turn increasing the potential for methanogenesis (Sanders et al., 2007 and references therein). As C_{org} content controlled benthic CH_4 production, it can be assumed that the silty-clayey content indirectly controlled CH_4 production and its subsequent flux (Fuchsman et al., 2015). However, organic-rich silty-clayey dominated sediments can result in higher CH_4 ebullition due to higher gas pressure build-up compared to sandy sediments (Chanton and Whiting, 1995). Bubble transport across the sediment-water interface was visually conspicuous at Amona (core A) and at Ganjem (core B) during the incubations whereas there was no indication of ebullition in Betim cores. Methane transported by these bubbles can escape oxidation in the sediments (Kiene, 1991; Chanton and Whiting, 1995) and accumulate in the overlying water leading to CH_4 supersaturation.

Methane production is carried out by a diverse group of methanogenic bacteria (Knittel and Boetius, 2009), and methanogenic archaea (Woese, 1987; Woese et al., 1990) which are strict anaerobes. The sediments in the Mandovi estuary were found to be dominated mainly by *Methanomicrobia* – a methanogenic archaea along with other archaea such as *methanobacteria*, *methanococci* and *methanopyri* (Khandeparkar et al., 2017). Phylogenetic analysis by Singh et al. (2010) have also revealed higher diversity of methanotrophic archaeal assemblages. Microbial studies in the mangrove sediments by Fernandes et al. (2014) in the estuary implies that the abundance and diversity of the microbial population not only depends on salinity but also on other factors like anthropogenic influence, mangrove dominance which play significant roles in the microbial community structure of the estuarine sediments and ecosystem functioning (Khandeparkar et al., 2017). Thus, the abundance of both methanogens and methanotrophs apparently controlled the CH₄ dynamics in the estuarine sediments and its benthic release.

4.2. Potential fluxes and methane oxidation

In the poisoned cores (Core E), CH₄ was released solely by diffusive transport from deeper sediment as CH₄ production in the top sediment layer and its oxidation at sediment-water interface were inhibited by HgCl₂ which arrested biological activity in these zones. These CH₄ fluxes represent the potential CH₄ flux in the absence of any biological consumption/oxidation of CH₄ in the sediments. The potential benthic fluxes of CH₄ from the Mandovi estuary were 1.6 to ~16 times higher than the measured fluxes implying high methanotrophic activity. Significant difference in the CH₄ flux rates between the poisoned cores and unpoisoned (anaerobic) cores indicated very high rates of CH₄ oxidation presumably carried out by methanotrophic bacteria or archaea at all three sites. The CH₄ oxidation varied along the salinity gradient. At the marine end the CH₄ oxidation rate was 17.10 $\mu\text{mol m}^{-2} \text{d}^{-1}$, while at Amona, the CH₄ oxidation rate was 10.30 $\mu\text{mol m}^{-2} \text{d}^{-1}$. The freshwater site showed the maximum rate of CH₄ oxidation of 1364.5 $\mu\text{mol m}^{-2} \text{d}^{-1}$. This is similar to observations from the Hudson estuary, where salinity appeared to have a significant influence on the spatial variability of CH₄ oxidation, with higher oxidation rates occurring towards the freshwater end (De Angelis and Scranton, 1993). Positive correlation of CH₄ oxidation with salinity ($r^2 = 0.78$; Fig. 9) is supportive of the view that low salinity favoured methanotrophy, controlling benthic CH₄ release and its ultimate flux to the atmosphere.

4.3. Comparison with other estuarine systems

Studies carried out elsewhere employing intact core incubations did not cover the salinity range as extensively as was done in the present study. A comparative account of published results of

sediment-water CH₄ flux studies carried out in various estuaries is provided in Table 2. Porewater CH₄ concentrations and sediment-water CH₄ fluxes generally decrease from the freshwater end to the seawater end of an estuary (Borges and Abril, 2011, and references therein). For example, in the White Oak River estuary, measurements by Kelley et al. (1990) at two points having salinities of 0.2 and 18.9 ppt yielded benthic CH₄ fluxes of 17100 μmol m⁻² d⁻¹ and < 240 μmol m⁻² d⁻¹, respectively. However, departure from this expected pattern is not uncommon. For instance, in the Cape Lookout Bight, a shallow eutrophic, quiescent coastal bay, benthic CH₄ flux of 14100 μmol m⁻² d⁻¹ was recorded at high salinities (30 – 35 ppt) by Martens and Klump (1980). Intense sulphate reduction fuelled by extremely high organic loading at this site leads to depletion of SO₄²⁻ close to the surface, creating suitable conditions for methanogenesis and leading to CH₄ ebullition from the seafloor. Similarly, in the Randers Fjord (Denmark), benthic CH₄ flux ranging from 3 to 400 μmol m⁻² d⁻¹ at 17 – 23 ppt salinities appeared to be associated with microphytobenthos mats (diatoms) which provided substrates for methanogenesis, while at lower salinities (3 – 7 ppt) negative CH₄ fluxes (–19 to –353 μmol m⁻² d⁻¹) reflected intense CH₄ oxidation (Abril and Iversen, 2002). Observations by Sansone et al. (1998) in the Tomales Bay, a temperate estuary, yielded benthic CH₄ fluxes ranging from –0.1 to 16 μmol m⁻² d⁻¹ at salinities of 10 – 30 ppt. While the negative benthic CH₄ flux at lower salinity was apparently due to intense CH₄ oxidation, the cause of the high flux at the marine end could not be ascertained. Zhang et al. (2008) also reported low CH₄ flux of 1.7 to 2.2 μmol m⁻² d⁻¹ at salinities from 3 to 6 in the Changjiang (Yangtze River) estuary. Dissolved CH₄ concentrations in this estuary (2.71 - 89.2 nM) are substantially lower than those reported from the European estuaries (Upstill-Goddard et al., 2000; Middelburg et al., 2002) and also those occurring in the Mandovi estuary (Araujo et al., 2017). Apparently, low organic loading limits net microbial CH₄ production in this estuarine system (Zhang et al., 2008 and references therein).

Methane fluxes from the sediments to the overlying water obtained with other experimental methods were relatively higher (Martens and Klump, 1980; Kelley et al., 1990). Methane flux at the sediment-water interface was recently reported to be 20.9 (±3) and 25.1 (±4) μmol m⁻² d⁻¹ in Godavari and Krishna estuaries, respectively (Rao and Sarma, 2016). Another recent study in a stream at Sitka by Bednarik et al. (2015) yielded highly variable benthic CH₄ fluxes (0 to 12,590 μmol m⁻² d⁻¹) suggesting interplay of many factors affecting benthic fluxes that could vary among different sites. Thus, it is clear that the, sediment–water CH₄ fluxes show extreme heterogeneity from one system to another and even within the same system, responding to a wide range of biogeochemical and hydrological conditions.

The Mandovi estuary is a typical estuary along the Indian west coast which differs widely from the from most other estuarine systems in terms of geographical, hydrological settings and consequently, the estuarine system undergoes extreme change in physical, biogeochemical and ecological features in a year. During the SW monsoon, the entire Mandovi estuary behaves like a freshwater body but turns into a tidal dominated system during the dry season. However, our measurements were made during the dry season when the salinity gradient in the estuary was well established. The residence time of the estuarine water changes dramatically from 2 days in monsoon to 31 days in dry season. Being a shallow and well-mixed system, and located in a tropical set up, the temperature of the estuarine water column remains above 25°C (Maya et al., 2011; Araujo et al., 2017) throughout the year which possibly causes higher mineralization of OM. Unlike the other estuaries which are highly polluted being located in highly industrialized and urbanized countries, the Mandovi estuary is still considered to be relatively pristine as it receives lower amount of anthropogenic OM and nutrients (Maya et al., 2011) and high amount of fresh water discharge. Presence of mangrove forests along almost the entire length of estuary possibly results in similar amount of OM inputs on the spatial scale. Contrary to some estuaries, the Mandovi estuary never experiences eutrophication or harmful algal blooms which are known to increase the organic load. Consequently, the estuarine water column never experiences anoxia which is usually conducive for extremely high CH₄ accumulation. Another important characteristic of the Mandovi estuary is the high Fe and Mn content of sediments due to regional geology which implies that these metals play a more important role in anaerobic degradation of organic matter than most other estuarine systems. The biogeochemistry of each estuary remains different owing to the difference in geographical and hydrological conditions and thus the benthic CH₄ fluxes among various estuarine systems would be different owing to the dissimilarity in dominance of controlling factors and their magnitude.

4.4. Implications of CH₄ fluxes in the estuary

Our results clearly show that the estuarine waters receive substantial CH₄ fluxes from sediments, even though the sedimentary efflux varied geographically due to several factors. The net upward flux implies that CH₄ production exceeded its oxidation in the sediments at all the three stations. The total area-integrated benthic CH₄ flux from the Mandovi estuary was computed to be 9.79×10^6 g CH₄ yr⁻¹. The large benthic supply would thus be an important contributor to the observed high CH₄ supersaturation in the estuarine waters (Araujo et al., 2017).

The estuarine waters at Betim, Amona and Ganjem contained CH₄ in high concentrations (28, 140 and 360 nM, respectively) at the time of the sampling. Considering the well-mixed condition of the water column, the pelagic CH₄ inventory at the three sites was 112, 700 and 2160 μmol m⁻², respectively. This implies that the benthic CH₄ flux would replenish the pelagic CH₄ stock in 23.5 days at Betim, 43.7 days at Amona and 23 days at Ganjem. The relatively long benthic turnover time is most likely because of our assumption of diffusive transport under steady state. However, as the estuary is a dynamic environment, the effects of mixing in the natural setting ought to be considered. Also the flux via ebullition may be important. Moreover, in addition to the benthic flux, there are other sources of CH₄. As pointed out earlier, the estuary also receives CH₄-enriched run-off from its large catchment area dominated mostly by mangrove vegetation, paddy fields and human settlements. The mangrove swamp sediments and paddy field soils can be particularly favourable sites for anaerobic mineralization of OM through methanogenesis, thereby providing substantial quantities of CH₄ to the adjacent estuarine waters.

As the benthic CH₄ flux is primarily controlled by porewater SO₄²⁻, and sedimentary C_{org} and silt-clay contents, large seasonality of fluxes is expected. This is because the estuarine characteristics are greatly impacted by the summer monsoon when the salinity gradient disappears and the estuary becomes nearly a fresh water body with salinity <4. Moreover, the estuary receives much larger quantities of silty-clayey sediments and OM as compared to the dry periods. Thus, it is quite possible that during the monsoon, water column and sediment biogeochemistry of the entire estuary would be similar to that observed at Ganjem in the present study. As low salinity enhances methanogenesis and methanotrophy, both benthic CH₄ fluxes and CH₄ oxidation are expected to be higher particularly in the middle and lower parts of estuary and the total CH₄ flux will be much higher than observed in the present study. Such potential seasonal effect that would apply to all estuaries along the west coast still needs to be studied.

5. Conclusion

The present study aimed at quantifying benthic CH₄ fluxes in the Mandovi estuary during summer when low river flow and high tidal dominance resulted in a prominent salinity gradient along the length of the estuary. Porewater CH₄ concentrations were much higher than those in the overlying water column thereby driving the flux of CH₄ from the sediments to the water column. Benthic CH₄ fluxes were measured through a series of intact core incubations at three locations representing different regimes covering the entire salinity range of the estuary. The estuarine sediments were found to be important source of CH₄ to the water column, but relatively high turnover times implied

that contributions from other sources such as run-off from mangrove forests and agricultural fields should also be important. Methane fluxes showed large variability along the salinity gradient with a clear increasing trend from the marine to the freshwater end. Strong inverse correlation of the benthic CH₄ fluxes with SO₄²⁻ and positive correlation with sedimentary C_{org} suggest dominant control of salinity on methanogenesis. Sedimentary silt-clay content also exerted some control over CH₄ fluxes. The inferred CH₄ oxidation rates increased upstream indicating that that low salinity also favored methanotrophy thereby controlling benthic CH₄ release and its ultimate flux to the atmosphere. High rate of net benthic CH₄ release and patchy CH₄ ebullition could partly account for the high CH₄ supersaturation in the estuarine water which, in conjunction with other CH₄ sources, makes the Mandovi estuary a CH₄ emitter to the atmosphere. Future works should investigate benthic CH₄ fluxes and oxidation during the monsoon season and also quantify CH₄ inputs from other sources such as mangrove wetlands fringing the estuary, agricultural fields and sewage outfalls.

Acknowledgements.

The authors express their gratitude to the Director, CSIR-NIO for providing the facilities for this work. We are thankful to Mr. H.S. Dalvi, Mr. B.R. Thorat and Mr. Chandrasekhar Rao for their help in the core collection. We acknowledge Mr. Jonathan Lobo, Ms. Chetna Bhat and Dr. Michelle Fernandes for kind assistance in experimental set up. Ms. Kausar Bepari is specially acknowledged for her help in the experiment set up, sampling and analysis. We thank Ms. S. Karapurkar and Dr. P. Kessarkar for kindly carrying out organic carbon and sediment texture analyses. J. Araujo and R. Naik are grateful to the University Grants Commission and Council of Scientific & Industrial Research (CSIR), respectively, for providing doctoral research fellowships. Dr. A. Pratihary thanks CSIR for the Quick Hired Fellowship. We are grateful to two anonymous reviewers for their constructive review, comments and suggestions which greatly improved the quality of the manuscript. This study formed a part of J. Araujo's Ph.D. project and was in part funded by the Ministry of Earth Sciences through the SIBER India project. This is NIO's contribution no. xxxx.

References

- Abril, G., Iversen, N., 2002. Methane dynamics in a shallow non-tidal estuary (Randers Fjord, Denmark). *Marine Ecology Progress Series*. 230, 171–181.
- Alongi, D.M., Wattayakorn, G., Pfitzner, J., Tirendi, F., Zagorskis, I., Brunskill, G.J., Davidson, A., Clough, B.F., 2001. Organic carbon accumulation and metabolic pathways in soil of mangrove forests in Southern Thailand. *Marine Geology*. 179, 85–103.

- Ansari, Z.A., Parulekar, A.H., 1993. Distribution, abundance and ecology of the meiofauna, in a tropical estuary along the west coast of India. *Hydrobiologia* 262, 47–56.
- Ansari, Z. A., Sivadas, S., Ingole, B. S., 2007. 'Benthic macrofauna', in *The Mandovi and Zuari Estuaries*, Shetye S. R., Kumar D., and Shankar D., Eds., p. 91-98, National Institute of Oceanography, Goa, India.
- Araujo, J., Naqvi, S.W.A., Naik, H., Naik, R., 2017. Biogeochemistry of methane in a tropical monsoonal estuarine system along the west coast of India, *Estuarine, Coastal and Shelf Science* doi: 10.1016/j.ecss.2017.07.016.
- Bange, H.W., Bartell, U.H., Rapsomanikis, S., Andreae, M.O. 1994. Methane in the Baltic and North Seas and a reassessment of the marine emissions of methane. *Global Biogeochemical Cycles* 8: 465-480.
- Baulch, H.M, Dillon. P.J, Maranger. R, Schiff. A.L., 2011. Diffusive and ebullitive transport of methane and nitrous oxide from streams: Are bubble-mediated fluxes important? *Journal of Geophysical Research*. 116, G04028.
- Bednarik, A., Cap, L., Maier, V., Rulik, M., 2015. Contribution of Methane Benthic and Atmospheric Fluxes of an Experimental Area (Sitka Stream). *Clean soil, air water*. DOI: 10.1002/clen.201300982.
- Blair, N.E., Aller, R.C., 1995. Anaerobic methane oxidation on the Amazon shelf. *Geochimica et Cosmochimica Acta* 59, 3707–3715.
- Borges, A. V., and Abril, G 2011. Carbon dioxide and methane dynamics in estuaries, p. 119–161. In W. Eric and M. Donald [eds.], *Treatise on estuarine and coastal science*. Academic Press.
- Bridgman, S.D., Cadillo-quiroz. H., Keller, J.K., Zhuang. Q. 2013. Methane emissions from wetlands: biogeochemical, microbial, and modeling perspectives from local to global scales. *Global Change Biology*, doi: 10.1111/gcb.12131
- Capone, D., R, Kiene., 1988. Comparison of microbial dynamics in marine and freshwater sediments: Contrasts in anaerobic carbon catabolism. *Limnology and Oceanography* 33:725-749.
- Canfield, D.E., B. Thamdrup, J.W. Hansen., 1993a. The anaerobic degradation of organic matter in Danish coastal sediments: iron reduction, manganese reduction, and sulphate reduction. *Geochimica et Cosmochimica Acta* 57 (16): 3867–3883.
- Canfield, D.E., B.B. Jorgensen., H. Fossing., R. Glud., J. Gundersen., N.B. Ramsing., B, Thamdrup., J.W. Hansen., L.P. Nielsen., and P.O.J. Hall., 1993b. Pathways of organic-carbon oxidation in three continental margin sediments. *Marine Geology* 113(1–2): 27– 40.
- Chanton, J.P., Martens, C.S., Kelley, C.A., 1989. Gas transport from methane-saturated, tidal freshwater and wetland sediments. *Limnology and Oceanography* 34, 807–819.
- Chanton, J.P., Dacey J.W.H 1991. Effects of vegetation on methane flux, reservoirs and carbon isotopic composition. In: Sharkey T., Holland E and Mooney H. (eds) *Trace gas emission from plants*, pp 65-92. Academic Press San Diego.

- Chanton, J.P., Whiting G.J., 1995. Trace gas exchange in freshwater and coastal marine environments: ebullition and transport by plants. In: Matson P.A. and Harriss R.C. (eds.), *Biogenic trace gases: measuring emissions from soil and water*, Blackwell Science, Oxford, pp. 98–125.
- Cline, J. D., 1969. Spectrophotometric determination of hydrogen sulfide in natural waters. *Limnology Oceanography* 14:454-458.
- De Sousa, S.N., Sen Gupta, .R. 1986. Variations of dissolved oxygen in Mandovi and Zuari estuaries. *Indian Journal of Marine Science*, vol. 15, pp. 67-71.
- De Angelis, M. A., Scranton, M. I., 1993. Fate of methane in the Hudson river and estuary, *Global Biogeochemical Cycles*7, 509–523.
- Deborde, J., Anschutz, P., Guerin, F., Poirier, D., Marty, D., Boucher, G., Thouzeau, G., 2010. Methane sources, sinks and fluxes in a temperate tidal Lagoon: The Arcachon lagoon (SW France), *Estuarine Coastal and Shelf Science* 89, 256–266.
- Dutta, M.K., Mukherjee R., Jana, T.K., Mukhopadhyay, S.K. 2015. Biogeochemical dynamics of exogenous methane in an estuary associated to a mangrove biosphere; The Sundarbans, NE coast of India. *Marine Chemistry* 170, 1-10.
- Folk, R.L., 1968. *Petrology of sedimentary rocks*, Hemphils, Drawer's M. University station, Austin, Texas, pp. 170.
- Fuchsman C.A., Devol A.H, Chase Z., Reimers C.E. , Hales B. 2015. Benthic fluxes on the Oregon shelf. *Estuarine, Coastal and Shelf Science* 163, 156-166.
- Gar'kusha, D.N., Fedorov, Yu. A., Khromov, M.I., 2010. Methane in the water and bottom sediments of the mouth area of the Severnaya Dvina river (White Sea), *Oceanology* 50, 498–512.
- Hammond, D. E., Cummins, K. M., McManus, J., Berelson, W. M., Smith, G., and Spagnoli, F., 2004. Methods for measuring benthic nutrient flux on the California Margin: Comparing shipboard core incubations to in-situ lander results, *Limnology Oceanography*.-Methods., 2, 146–150.
- Huttunen, J.T., Vaisanen .T.S., Hellsten., S.K., Martikainen, P.J., 2006. Methane flux at the sediment-water interface in some boreals lakes and reservoirs. *Boreal Environment research* 11, 27-34.
- Jayakumar, D. A., Naqvi, S. W. A., Narvekar, P. V., George, M. D., 2001. Methane in coastal and offshore waters of the Arabian Sea. *Marine Chemistry* 74, 1–13.
- Jørgensen, B.B., Weber, A., Zopfi, J., 2001. Sulfate reduction and anaerobic methane oxidation in Black Sea sediments. *Deep-Sea Research Part I-Oceanographic Research Papers* 48, 2097-2120.
- Khandeparker .L., Kuchi.N., Kale,D., Anil.A.C 2017. Microbial community structure of surface sediments from a tropical estuarine environment using next generation sequencing *Ecological Indicators*, vol.74; 172-181.
- Kelley, C.A., Martens, C.S., Chanton, J.P., 1990. Variations in sedimentary carbon remineralization rates in the White Oak River estuary, North Carolina. *Limnology and Oceanography* 35 (2), 372-383.

- Kelley, C.A., Martens, C.S, Ussler, W. III., 1995. Methane dynamics across a tidally flooded riverbank margin. *Limnology Oceanography* 40:1112–1129
- Knittel, K., Boetius, A., 2009. Anaerobic oxidation of methane: progress with an unknown process. *Annual Review of Microbiology* 63, 311-334.
- Kiene R.P. 1991. Production and consumption of methane in aquatic systems. In: Rogers J.E. & Whitman W.B. (eds.), *Microbial production and consumption of greenhouse gases: methane, nitrogen oxides, and halomethanes*, American Society for Microbiology, Washington, D.C., pp. 111–146.
- Krüger, M., Treude, T., Wolters, H., Nauhaus, K., Boetius, A., 2005. Microbial methane turnover in different marine habitats. *Palaeogeography, Palaeoclimatology, Palaeoecology* 227, 6-17.
- Krishna Kumari, L., Bhattathiri, P.M.A., Matondkar, S.G.P., John, J., 2002. Primary productivity in Mandovi-Zuari estuaries in Goa. *Journal of Marine Biological Association of India* 44, 1–13.
- Lilley, M. D., de Angelis M. A., Olson J. E., 1995. Methane concentrations and estimated fluxes from Pacific Northwest rivers, *Mitt. Int. Ver. Theor. Angew. Limnol.* 25, 187–196.
- Longhi, D., Bartoli, M., Nizzoli, D., Viaroli, P., 2013. Benthic processes in fresh water fluffy sediments undergoing resuspension *Journal of Limnology* 72(1): 1-12.
- Martens, C. S., R. A. Berner., 1974. Methane production in sulphate-depleted marine sediments. *Science* 18: 1167–1169. doi:10.1126/science.185.4157.1167.
- Martens, C. S., Klump, J. V., 1980. Biogeochemical cycling in an organic-rich coastal marine basin. I. Methane sediment water exchange processes. *Geochimica Cosmochimica Acta* 44, 471–490.
- Martens, C.S., 1982. Methane production, consumption, and transport in the interstitial waters of coastal marine sediments. *The Dynamic Environment of the Ocean Floor*, 187-202.
- Martens, C. S., D. B. Albert, and M. J. Alperin. 1998. Biogeochemical processes controlling methane in gassy coastal sediments - part 1. A model coupling organic matter flux to gas production, oxidation and transport. *Continental Shelf Research* 18: 1741–1770. doi:10.1016/S0278-4343(98)00056-9
- Maya, M.V., Soares, M.A., Agnihotri, R., Pratihary, A.K., Karapurkar, S., Naik, H., Naqvi, S.W.A., 2011. Variations in some environmental characteristics including C and N stable isotopic composition of suspended organic matter in the Mandovi Estuary. *Environmental Monitoring and Assessment*. 175, 501–517
- McAuliffe, C., 1971. GC determination of solutes by multiple phase equilibration. *Chemical Technology*, 1, 46–50.
- Middelburg, J.J., Klaver, G., Nieuwenhuize, J., Wielemaker, A., Haas, W., Vlut, T., Van der Nat, F.J.W.A., 1996. Organic matter mineralization in intertidal sediments along an estuarine gradient. *Marine Ecology Progress Series* 132, 157–168.

- Middelburg, J.J., Nieuwenhuize, J., Iversen, N., Høgh, N., de Wilde, H., Helder, W., Seifert, R., Christof, O., 2002. Methane distribution in tidal estuaries. *Biogeochemistry* 59, 95–119.
- Miller-Way, T., Boland, G. S., Twilley, R. R., 1994. Sediment oxygen consumption and benthic nutrient fluxes on the Louisiana continental shelf: A methodological comparison, *Estuaries*, 17, 809–815.
- Musenze R.S., Werner, U., Grinham, A., Udy, J., Yuan, Z., 2014. Methane and nitrous oxide emissions from a subtropical estuary (the Brisbane River estuary, Australia). *Science of Total Environment*; 472:719–29.
- Pai, S., Gong, G., Liu, K., 1993. Determination of dissolved oxygen in seawater by direct spectrophotometry of total iodine. *Marine Chemistry* 41, 343–351.
- Pratihary, A.K., Naqvi, S.W.A., Naik, H., Thorat, B.R., Narvenkar, G., Manjunatha, B.R., Rao, V. P., 2009. Benthic fluxes in a tropical estuary and their role in ecosystem. *Estuarine Coastal Shelf Science* 85, 387–398.
- Pratihary, A.K; Naqvi, S.W.A, Narvenkar, G, Kurian, S., Naik, H., Naik, R., Manjunatha, B.R., 2014. Benthic mineralization and nutrient exchange over the inner continental shelf of western India. *Biogeosciences* 11, 2771–2791.
- Pradeep Ram, A.S., Nair, S., Chandramohan, D., 2003. Seasonal shift in net ecosystem production in a tropical Estuary. *Limnology and Oceanography* 48, 1601–1607.
- Qasim, S.Z., Sen Gupta, R., 1981. Environmental characteristics of the Mandovi-Zuari estuarine system in Goa. *Estuarine Coastal Shelf Science* 13, 557-578.
- Rao, G.D., Sarma, V.V.S.S., 2016. Variability in concentrations and fluxes of methane in the Indian estuaries. *Estuaries and Coasts* DOI 10.1007/s12237-016-0112-2.
- Reshmi, R.R., Deepa Nair, K., Zachariah, E. J., Vincent, S.G.T., 2014. Methanogenesis: Seasonal changes in human impacted regions of Ashtamudi estuary (Kerala, South India), *Estuarine, Coastal and Shelf Science*, <http://dx.doi.org/10.1016/j.ecss.2014.11.031>.
- Sansone, F. J., Rust, T. M., Smith, S. V., 1998. Methane distribution and cycling in Tomales bay, California. *Estuaries*, 21, 66 –77
- Sanders, I.A., Heppell, C.M., Cotton, J. A., Wharton, G., Hildrew, A., Flowers, E. J., Trimmer, M., 2007. Emissions of methane from chalk streams has potential implications for agricultural practices, *Freshwater Biology* 52, 1176 –1186.
- Seeberg-Elverfeldt, J., Schlüter, M., Feseker, T., Kölling, M. 2005. Rhizon sampling of porewaters near the sediment-water interface of aquatic systems. *Limnology and Oceanography: Methods* 3, 361–371.
- Singh, S.K., Verma, P., Ramaiah, N., Chandrashekar, A.A., Shouche, Y.S., 2010. Phylogenetic diversity of archaeal 16S rRNA and ammonia monooxygenase genes from tropical estuarine sediments on the central west coast of India. *Res. Microbiol.* 161, 177-186.

Smith, B.N., and Epstein, S., 1971. Two categories of $\delta^{13}\text{C}/\delta^{12}\text{C}$ ratios for higher plants. *Plant Physiology* 47, 380-384.

Treude, T., Krüger, M., Boetius, A., Jørgensen, B.B., 2005. Environmental control on anaerobic oxidation of methane in the gassy sediments of Eckernförde Bay (German Baltic). *Limnology and Oceanography* 50, 1771-1786.

Upstill-Goddard, R.C., Barnes, J., Frost, T., Punshon, S., Owens, N.J.P., 2000. Methane in the southern North Sea: low-salinity inputs, estuarine removal and atmospheric flux. *Global Biogeochemical Cycles* 14:1205–1217.

Valentine, D., 2002. Biogeochemistry and microbial ecology of methane oxidation in anoxic environments: a review. *Antonie Van Leeuwenhoek* 81, 271–282.

Van der Nat FJWA., de Brouwer, J.C.F., Middelburg, J.J., Laanbroek, H.J., 1997. Spatial distribution and inhibition by ammonium of methane oxidation in intertidal freshwater marshes. *Applied Environmental Microbiology* 63:4734 – 4740.

Vijith, V., Sundar, D., Shetye, S.R., 2009. Time-dependence of salinity in monsoonal estuaries. *Estuarine Coastal Shelf Science* 85, 601-608.

Wafar, S., Untawale, A.G., Wafar, M., 1997. Litter fall and energy flux in a Mangrove ecosystem. *Estuarine, Coastal and Shelf Science* 44, 111–124.

Woese, C.R., 1987. Bacterial evolution. *Microbiol. Rev.* 51, 221-271.

Woese, C.R., Kandler, O., Wheelis, M.L., 1990. Towards a natural system. *Proc. Natl. Acad. Sci. U. S. A.* 87, 4576-4579.

Woulds, C., Schwartz, M. C., Brand, T., Cowie, G. L., Law, G., Mowbrey, S. R. 2009. Porewater nutrient concentrations and benthic nutrient fluxes across the Pakistan margin OMZ, *Deep-Sea Research. Pt. II*, 56, 333–346.

Zhang, G., Zhang, J., Liu, S., Ren, J., Xu, J., Zhang, F., 2008. Methane in the Changjiang (Yangtze River) Estuary and its adjacent marine area: Riverine input, sediments release and atmospheric fluxes. *Biogeochemistry* 91, 71–84.

Figures

Fig.1. Map of the study area showing the location of the sampling sites (red dots).

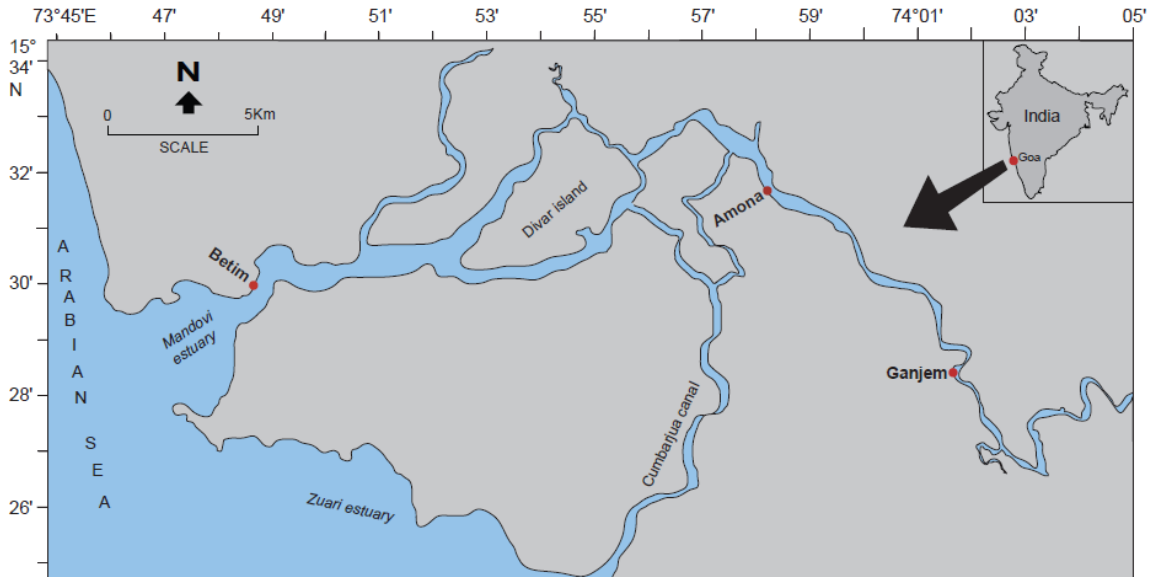


Fig. 2. Experimental set up of the intact-core incubation.

Fig.2

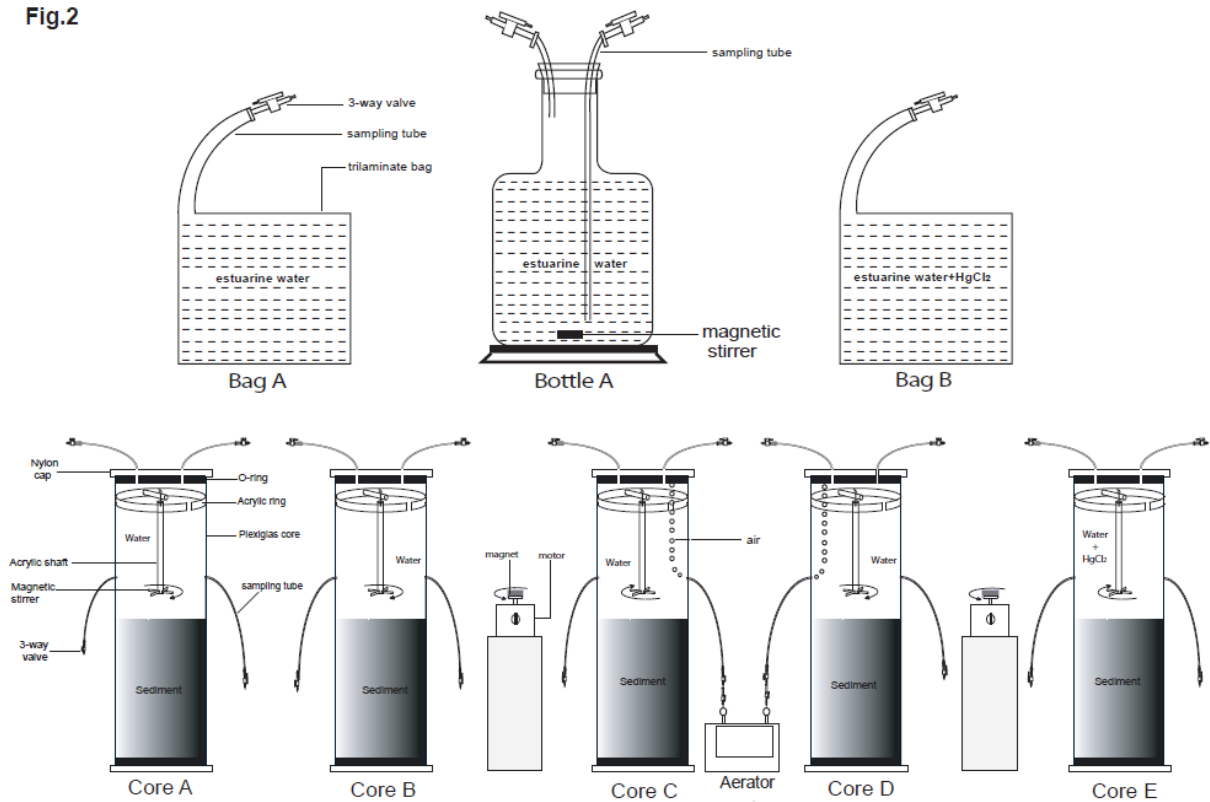


Fig. 3. Downcore variations of (a) porosity and sediment texture at (b) Betim (c) Amona, and (d) Ganjem.

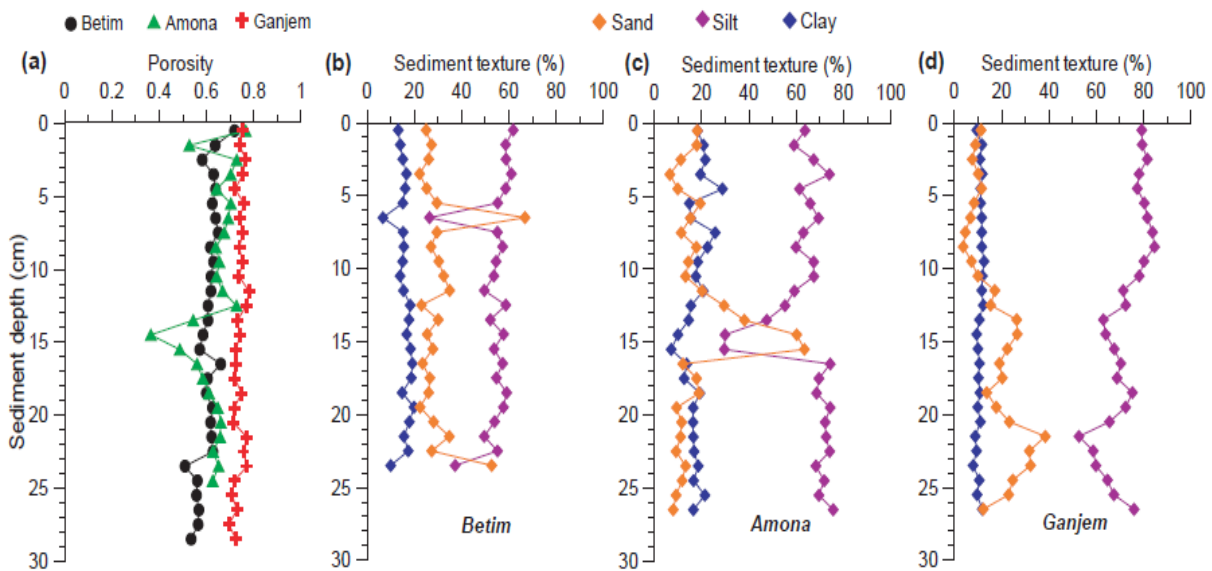


Fig.4. Downcore variations of (a) porewater SO_4^{2-} and (b) sedimentary organic carbon (c) porewater CH_4 .

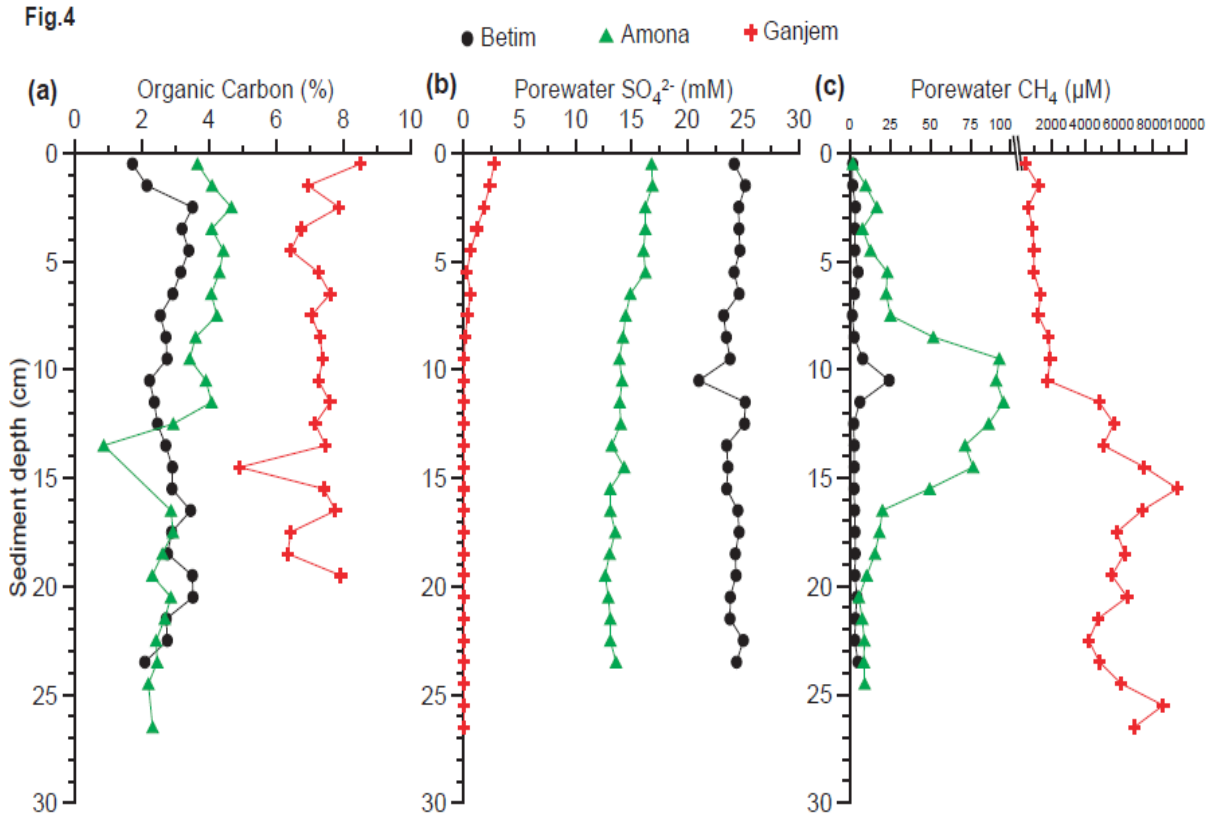


Fig. 5. Variation of (a) DO and (b) CH_4 with time in the cores from Betim during the incubation.

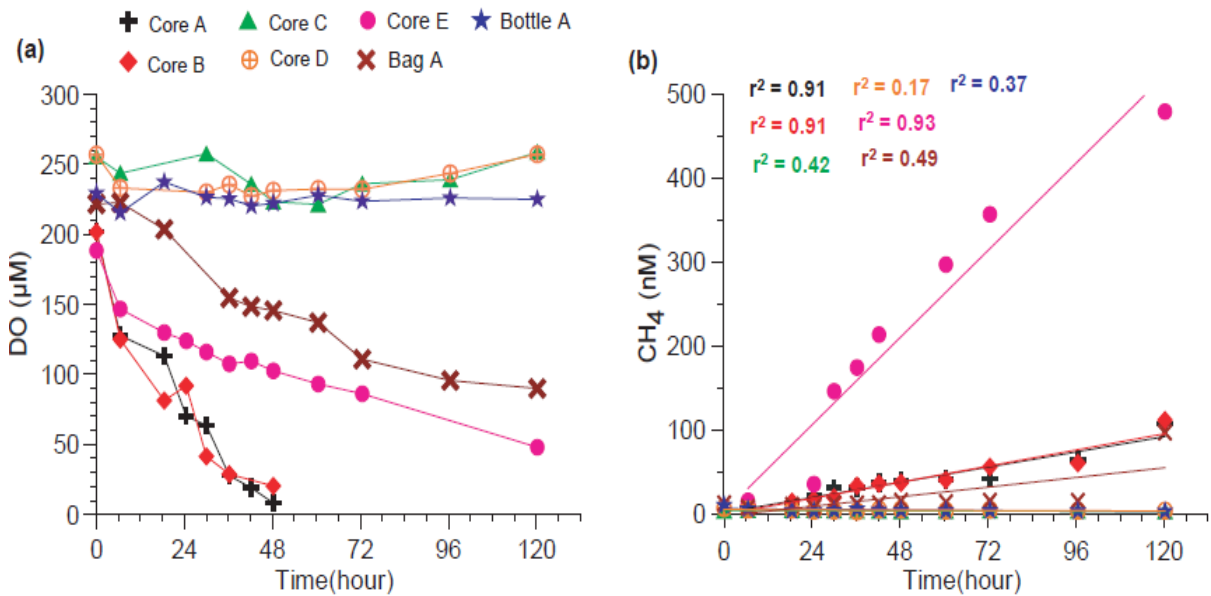


Fig.6. Variation of (a) DO and (b) CH_4 with time in the cores from Amona during the incubation. The encircled + values were due to ebullition effect (b.1) CH_4 in headspace with time in core A.

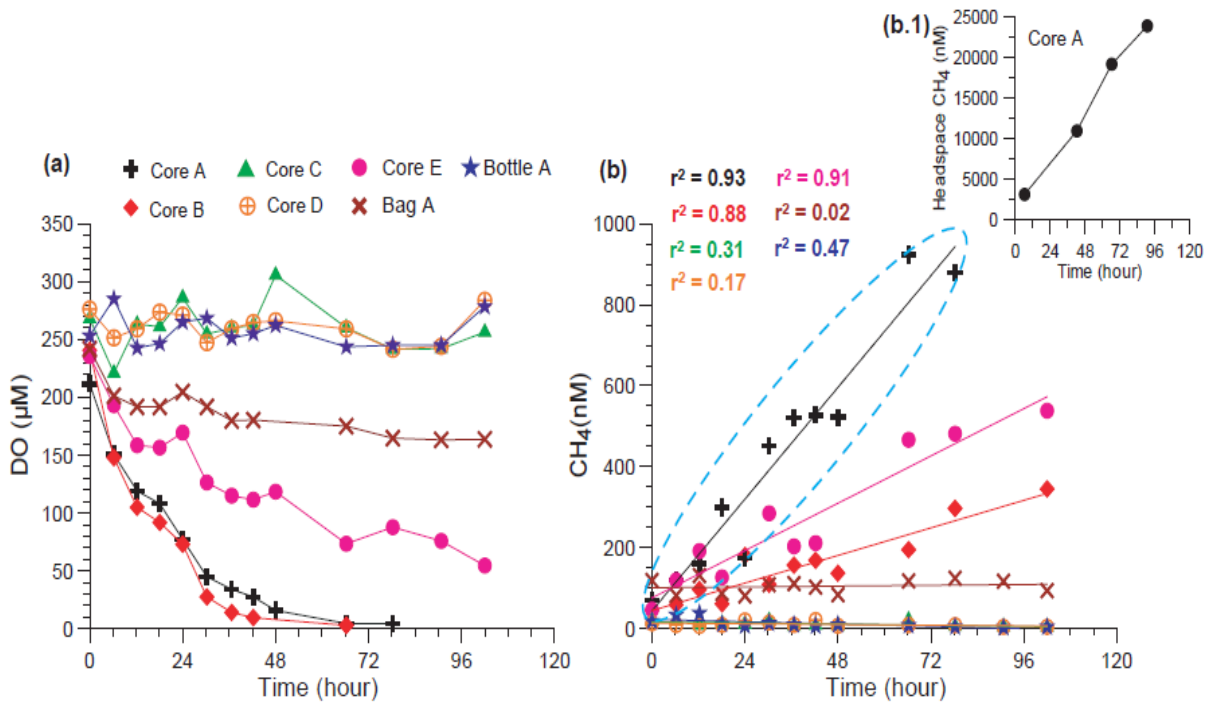


Fig.7. Variation of (a) DO and (b) CH_4 with time in the cores from Ganjem during the incubation. The encircled values were due to ebullition effect (b.1) CH_4 in headspace with time in core B.

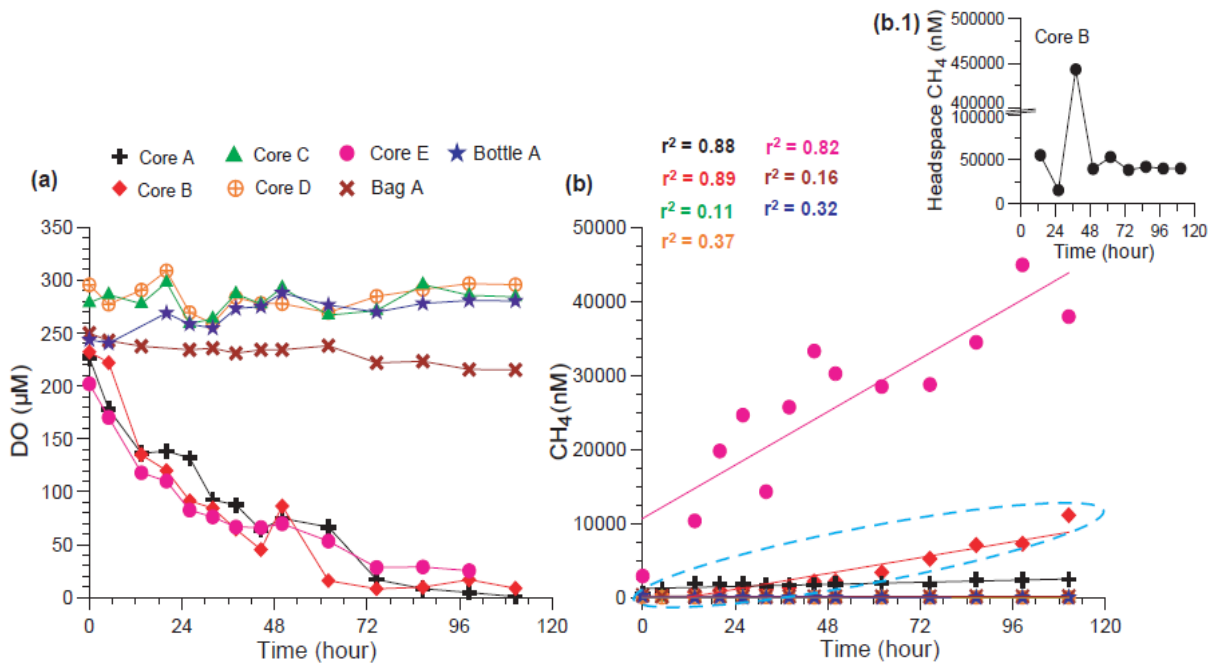


Fig. 8. Correlation between (a) CH₄ flux and porewater CH₄ vs salinity (b) CH₄ flux and porewater CH₄ vs porewater sulphate (c) CH₄ flux and porewater CH₄ vs C_{org} of surficial sediments (d) CH₄ flux and porewater CH₄ vs % of Silt+Clay of surficial sediments.

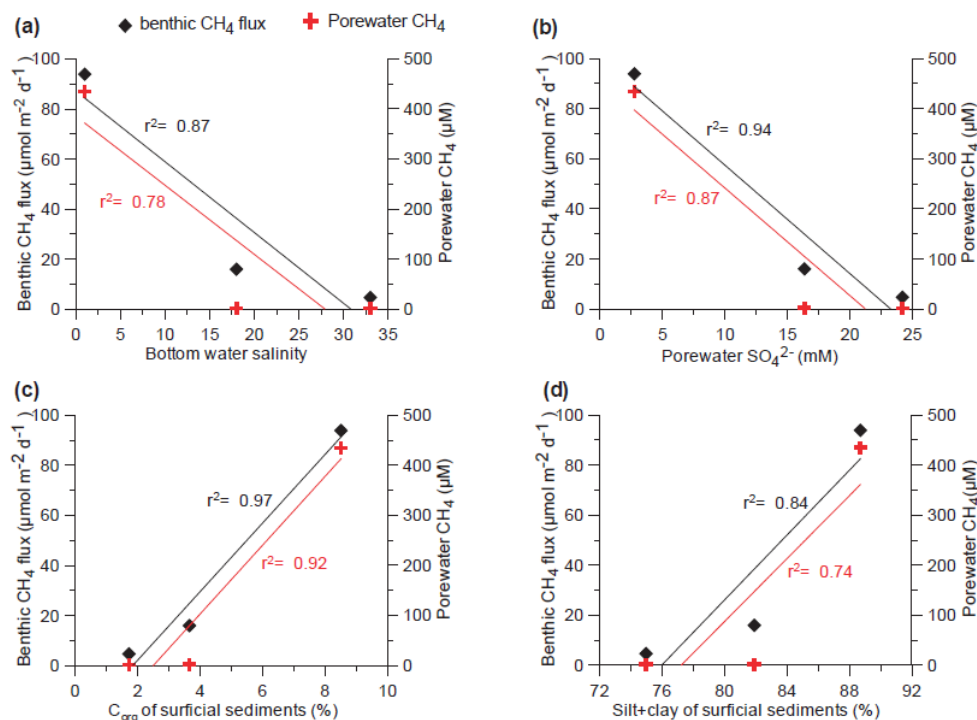
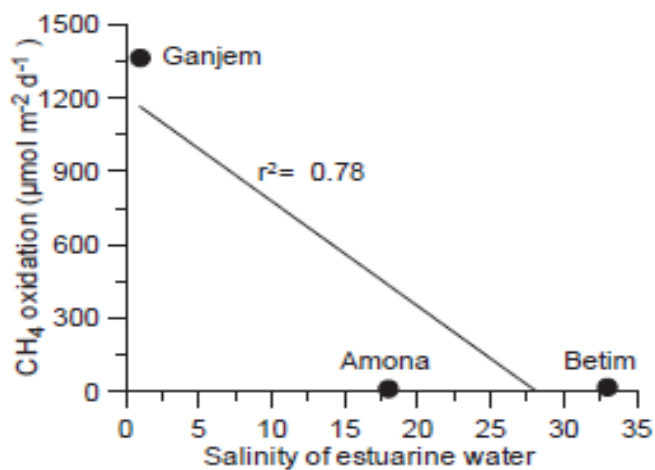


Fig. 9. Correlation between CH₄ oxidation rates and salinity.



Tables

Table 1. Details of whole core incubations in the Mandovi estuary. Values in parenthesis are standard deviation for the average flux rate from replicate cores. No linear CH₄ accumulation was observed in Bag A, Bottle A and Bag B and thus rates could not be calculated.

System	description	Mode of incubation	Duration of incubation (h)	Sampling interval (h)	Benthic CH ₄ fluxes ($\mu\text{mol m}^{-2} \text{d}^{-1}$)		
					Betim (Lower estuary)	Amona (mid estuary)	Ganjem (Upper estuary)
Bag-A	Estuarine bottom water	anaerobic	120	6-12	----	----	----
Core-A, Core-B	Estuarine sediment+bottom water	anaerobic	120	6-12	4.75 (± 0.007)	16.01	93.90
Bottle-A	Estuarine bottom water	aerobic	120	6-12	----	----	----
Core-C, Core-D	Estuarine sediment+bottom water	aerobic	120	6-12	-0.065 (± 0.021)	-0.56 (± 0.21)	-1.08 (± 1.20)
Bag-B	Estuarine bottom water	anaerobic + poisoned	120	6-12	----	----	----
Core-E	Estuarine sediment+bottom water	anaerobic + poisoned	120	6-12	21.80	26.31	1449.39

Table 2. Comparison between the sediment–water CH₄ fluxes ($\mu\text{mol m}^{-2} \text{d}^{-1}$) with corresponding salinity in different estuarine systems of the world.

Study Area	Salinity (psu)	Methodology	Benthic CH ₄ flux rate ($\mu\text{mol m}^{-2} \text{d}^{-1}$)	Reference
Cape Lookout Bight	30 – 35	Benthic chamber	14100	Martens and Klump (1980)
White Oak River estuary	0.2	Calculation from porewater profiles + benthic chamber	17100	Kelley et al. (1990)
	18.9		< 240	
Tomales Bay	10 – 36	Benthic chamber	– 0.1 to 16	Sansone et al. (1998)
Randers Fjord estuary	3 – 7	Intact core incubation	– 19 to – 353	Abril and Iverson (2002)
	17 – 23		3 to 400	
Yangtze estuary	3 – 6	Intact core incubation	1.7 to 2.2	Zhang et al. (2008)
Mandovi estuary	1-33	Intact core incubation	4.75 to 93.9	Present study